Composites Part B 171 (2019) 146–153

Contents lists available at ScienceDirect

Composites Part B

journal homepage: www.elsevier.com/locate/compositesb

Mechanism of greatly increasing dielectric constant at lower percolation thresholds for epoxy resin composites through building three-dimensional framework from polyvinylidene fluoride and carbon nanotubes

Ningning Zhu, Li Yuan, Guozheng Liang *, Aijuan Gu **

State and Local Joint Engineering Laboratory for Novel Functional Polymeric Materials, College of Chemistry, Chemical Engineering and Material Science, Soochow University, Suzhou, 215123, China

ARTICLE INFO

Keywords:
Polymer-matrix composites (PMCs)
3-Dimensional reinforcement
Thermosetting resin
Electrical properties

ABSTRACT

Achieving higher dielectric constant (*Dk*) at lower conductor content is an interesting challenge for developing high-*Dk* composites. Herein, novel 3D-framework (fPCNT) from polyvinylidene fluoride (PVDF) and carbon nanotubes (CNTs) was prepared, which was infiltrated with epoxy (EP) resin to fabricate new composites (fPCNT/EP). The crystalline phase, spatial distribution and interfacial interaction of fPCNT were discussed, and dielectric properties of fPCNT/EP were compared with those of traditional filler embedded composites (CNT/EP and CNT/PVDF/EP) and four composites (M450-CNT/EP, M20-CNT/EP, CNa-CNT/EP and CC-CNT/EP) based on 3D-frameworks from CNTs and traditional cellulose binders. fPCNT/EP not only has much lower percolation threshold ($f_c = 0.25$ wt%) and higher *Dk* at f_c (170, 100 Hz) than CNT/EP and CNT/PVDF/EP, but also shows higher *Dk* and better *Dk*-frequency stability than M450-CNT/EP, M20-CNT/EP, CNa-CNT/EP and CC-CNT/EP composites with same CNT contents. The mechanism behind was intensively investigated through building structure-property relationship.

1. Introduction

Polymer composites with high dielectric constant (*Dk*) have important applications in new energy, information technology and insulated electrical fields owing to their light weight, excellent process ability, good storage and uniform electric field capability [1–4]. The greatest advantage of conductor/polymer composites is their higher *Dk* at small conductor loadings. As the conductor content (*f*) approaches percolation threshold (f_c), *Dk* will jump to a high value, while the dielectric loss continues to increase as *f* increases. Various methods such as surface modification [5,6], coating and functionalization [7,8] of conductors have been adopted to reduce dielectric loss of composites, however, these methods usually reduce the conductivity of conductors, leading to increased f_c, and thus degraded process feature and cost.

To reduce f_c, orientation of conductors in polymer matrix is a good method, which also tends to achieve high *Dk* and low dielectric loss [9]. Orientation methods mainly include utilizing electric field [10], magnetic field [11], shearing and stretching [12], electrospinning [13] and microwave curing [9], however, they have additional requirements on polymer or conductors. For example, materials that can respond to electric and magnetic fields should be introduced on the surface or entered into the internal part of conductors [11,14]; while microwave orientation process is not easy to be controlled and only suitable for some thermosetting resins [15].

In recent years, ice template method has been used to prepare porous or textile polymers [16], ceramics [17], bioglass [18], conductor [19] and so on. Most studies focused on studying the effect of three-dimensional structures on properties of composites, but no studies about dielectric properties based on conductor framework has been reported so far.

Compared with other properties, dielectric properties of a composite are very sensitive to the composition. Binder is the necessary and important component of three-dimensional framework, the most commonly used binders for preparing framework are methyl cellulose [20] and polyvinyl alcohol [21]; however their role is adhesion of bonding fillers, but almost makes no contribution to high *Dk* for composites. Therefore, it is particularly important to select a polymer with excellent dielectric properties. Among all polymers, polyvinylidene

* Corresponding author
** Corresponding author.
E-mail addresses: lgzheng@suda.edu.cn (G. Liang), ajgu@suda.edu.cn (A. Gu).

https://doi.org/10.1016/j.compositesb.2019.04.042
Received 21 January 2019; Received in revised form 9 April 2019; Accepted 29 April 2019
Available online 2 May 2019

fluoride (PVDF) is a special semi-crystalline polymer that exhibits high *Dk* (~10), low dissipation factor and high dielectric strength [22,23], which has been widely used to prepare high *Dk* composites [24].

In this paper, a unique 3D-framework (fPCNT) based on PVDF and CNTs was developed using ice template method, which was then infiltrated with epoxy resin (EP) to prepare new composites (fPCNT/EP), of which dielectric properties and mechanism behind were systematically studied and compared with those of traditional filler embedded composites (CNT/EP and CNT/PVDF/EP). In addition, the effect of binder nature on dielectric properties of composites was studied.

2. Experimental

2.1. Materials

CNTs with a purity of more than 97% (the average out diameter is 7–15 nm, and the length is greater than 5 μm) were bought from Shenzhen Nanoport Company, China. EP resin was diglycidyl ether of bisphenol A, purchased from Wuxi Resin Plant, China, of which the epoxide equivalent weight was 196 g/mol. 1,4-Dioxane was obtained from Sinopharm Group Chemical Reagent Suzhou Co., Ltd., PVDF powders (density = 1.77 g/cm^3) were supplied by Solvay Company of France. Methylhexahydrophthalic methyl hexahydrophthalic anhydride (MHHPA), tetrabutylammonium bromide (TBAB, 99%), methyl cellulose (M450), methyl cellulose (M20), sodium carboxymethyl cellulose (CNa) and carboxymethyl cellulose (CC) were all commercial products.

2.2. Preparation of CNT frameworks

1.4 g of PVDF powders and 68.6 g of 1, 4-dioxane were blended with stirring at 70 °C for 24 h to obtain PVDF solution. CNT/PVDF suspension was prepared by adding 0.1 wt%, 0.2 wt%, 0.22 wt%, 0.25 wt%, 0.30 wt % or 0.35 wt% CNTs into the solution at room temperature, followed by mechanical stirring for 30 min and ultrasonic stirring for 20 min, successively. The resulting suspension was poured into a Teflon mold with copper sheet at the bottom, and then frozen at −70 °C for 6 h. After that, the mold was placed into a freeze dryer at −45 °C with 50 Pa for 24 h to obtain a three-dimensional framework, designated as fPCNT.

Pure PVDF framework (fPVDF) was prepared using the process for fPCNT, except that no CNTs were added. Besides, following the procedure for fPCNT, other binder such as M450, M20, CNa or CC was used to prepare different framework, which was coded as M450-CNT, M20-CNT, CNa-CNT or CC-CNT.

2.3. Preparation of CNT/EP and CNT/PVDF/EP composites

According to Table S1, EP and MHHPA (w/w = 52.7/44.8) were mixed with stirring at 80 °C for 20 min to obtain a resin, into which CNTs were added with ultrasonical stirring at 80 °C for 30 min, followed by adding TBAB with stirring at 80 °C for 20 min to get a prepolymer. The prepolymer was poured into a mold, and vacuum degassing at 80 °C. After that the mold was transferred into a blast oven and cured following the procedure of 100 °C/2h + 120 °C/2 h + 140 °C/4h, and then naturally cooled to obtain a CNT/EP composite, coded as m-x, wherein x is the content of CNTs in composite.

According to Table S1, PVDF powders were added into EP at 70 °C for 24 h and ultrasonically stirring for 30 min, successively. MHHPA was then added with stirring at 80 °C for 20 min to get a resin, into which CNTs were added with ultrasonical stirring at 80 °C for 30 min, followed by adding TBAB with stirring at 80 °C for 20 min to get a prepolymer. The prepolymer was then treated using the procedure for preparing CNT/EP composite as described above. The resulting CNT/PVDF/EP composite is coded as p-x, wherein x is the content of CNTs in composite.

2.4. Preparation of composites based on CNT frameworks

EP and MHHPA were mixed (w/w = 100/85) with stirring at 80 °C for 20 min to obtain a resin, into which TBAB was added with stirring at 80 °C for 20 min to get a prepolymer. The prepolymer was then treated using the procedure for preparing CNT/EP composite as described above. The resulting fPCNT/EP composite is designated as f-x. The detail compositions were listed in Table S1.

The composite based on M450-CNT, M20-CNT, CNa-CNT or CC-CNT was prepared using the similar method for fPCNT/EP, and coded as M450-CNT/EP, M20-CNT/EP, CNa-CNT/EP or CC-CNT/EP. The content of CNTs in each composite was 0.25 wt%.

2.5. Measurements

The crystal forms of PVDF were examined with an X-ray diffraction (XRD, Rigaku, Tokyo, Japan). A scanning electron microscope (SEM, Hitachi S-4700, Japan) was employed to observe morphologies of fracture surfaces of composites. Fourier transform infrared spectroscopy (FTIR, Nicolet 6700, thermoscientific USA) was used to record chemical bonds between PVDF and CNTs. Raman spectra were recorded using an Almega dispersive Raman spectrometer (Thermo Nicolet, Madison, WI), and the laser wavelength was selected as 514.5 nm. Dielectric and electric properties were measured on a broadband dielectrics spectrometer (Novocontrol Concept 80, Hundsangen, Germany) at room temperature, the dimensions of each sample were $(20 \pm 0.1) \times (20 \pm 0.1) \times (3 \pm 0.1)$ mm^3. Three-dimensional morphologies of composites were observed using an In Vivo Micro-Compute Tomography (model 1176) produced by SKYSCAN Co., Ltd, Belgium.

3. Results and discussion

3.1. Identification of crystalline phases of PVDF

PVDF is a semi-crystalline polymer that has five crystal forms, including α, β, γ, δ, and ε [22], PVDF with different crystal form has different dielectric properties, therefore it is crucial to confirm the crystal form of PVDF in each composite. XRD patterns can give direct information on the crystal forms of PVDF. As shown in Fig. 1, PVDF film and PVDF powders have same diffraction peaks of α-crystalline phase at 17.7° (100), 18.4° (020), 19.9° (110) and 26.6° (021) [25], suggesting that the film formation using 1, 4-dioxane as solvent does not change the crystal form of PVDF powders. fPVDF and fPCNT also have diffraction peaks at 17.7°, 18.4° and 26.6°, hence PVDF in the framework still has α crystal form. However, patterns of fPVDF and fPCNT do not show the diffraction peak at 19.9°, instead, exhibiting a new peak at 20.2° that belongs to the characteristic peak of β crystal form [26], meaning that both α and β crystal forms exist in fPVDF and fPCNT. In addition, the relative crystallinity of β crystal form in fPCNT is 35.8%, which is higher than that of fPVDF (Table S2), meaning that the presence of CNTs is helpful for the formation of β crystals. The reason behind is that the process of solvent icing in ice template method has certain directionality [27], resulting in transition of segment arrangement of PVDF.

To further confirm whether PVDF in composites has same crystal form, PVDF powders, fPVDF and fPCNT were treated with the same process for preparing composites, and then XRD patterns were recorded. As shown in Fig. 1b, XRD patterns of the sample after thermal treat is the same as that before heat treatment, meaning that the thermal history does not change the crystal form of PVDF.

3.2. Interfacial interaction of fPCNT framework

In order to understand the force between PVDF and CNTs in fPCNT, FTIR spectra of PVDF powders, fPVDF and fPCNT were recorded (Fig. 2a). The peaks reflecting –CH_2 (1379 and 1400 cm^{-1}), –CF_2 (1180 and 1147 cm^{-1}) and C–C (870 cm^{-1}) [28] are founded in all spectra.

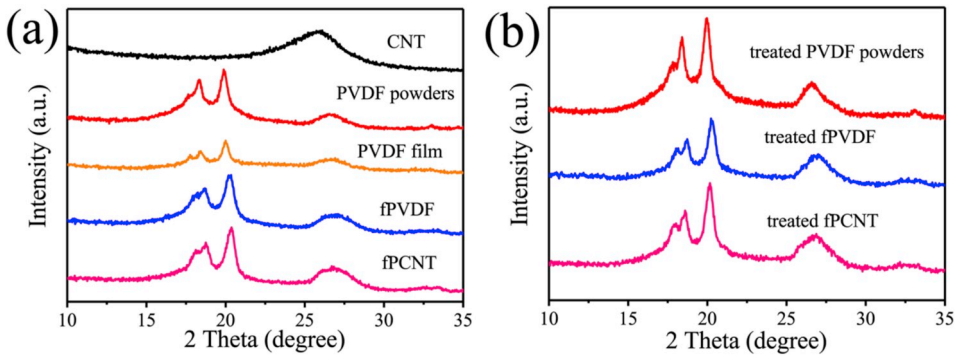

Fig. 1. XRD patterns of original (a) and thermally treated samples with curing process (b).

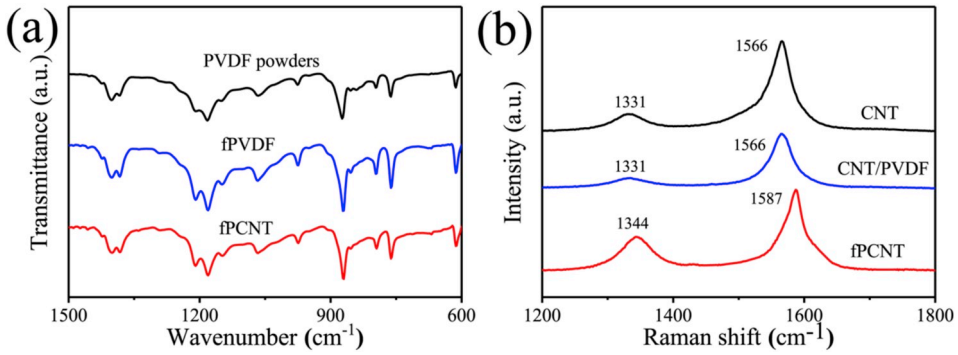

Fig. 2. FTIR spectra of PVDF powders, fPVDF and fPCNT (a); Raman spectra of CNTs, CNT/PVDF and fPCNT (b).

However, no new characteristic peaks appear in fPCNT spectrum compared to spectra of fPVDF and PVDF powders, indicating that PVDF and CNTs in fPCNTs are not linked by chemical bonds.

Above statement is further confirmed by Raman spectra. PVDF powders were dispersed in deionized water, followed by mechanically stirred at 70 °C for 24 h and ultrasonically stirred for 30 min, successively. CNTs (0.34 wt %) were then added with ultrasonical stirring at 80 °C for 30 min. The resulting mixture was putted into an oven to get off water for Raman tests. As shown in Fig. 2b, there are typical D-band peak (1331.9 cm^{-1}) and G-band peak (1566.1 cm^{-1}) in spectra of CNTs and CNT/PVDF. CNT/PVDF spectrum shows same peaks as spectrum of CNTs, suggesting that CNT and PVDF have not interaction in bad solvent. G and D band peaks also appear in the Raman spectrum of fPCNT, but they have red shifts of 21 cm^{-1} and 13 cm^{-1}, respectively. This is attributed to the formation of donor-acceptor complexes [29] and compressive forces of PVDF adsorbed on surfaces of CNTs [30] induced by the electron-rich property of CNTs and the electron deficient of PVDF. F atoms on PVDF molecule have strong electrophilicity, while CNT surfaces have a large amount of electrons, so F atoms of PVDF will form a donor-acceptor complexes with the delocalized π electron cloud on CNT surfaces in 1,4-dioxane. Above FTIR and Raman spectra prove that PVDF and CNTs in fPCNT have electron attraction, but not chemical bond.

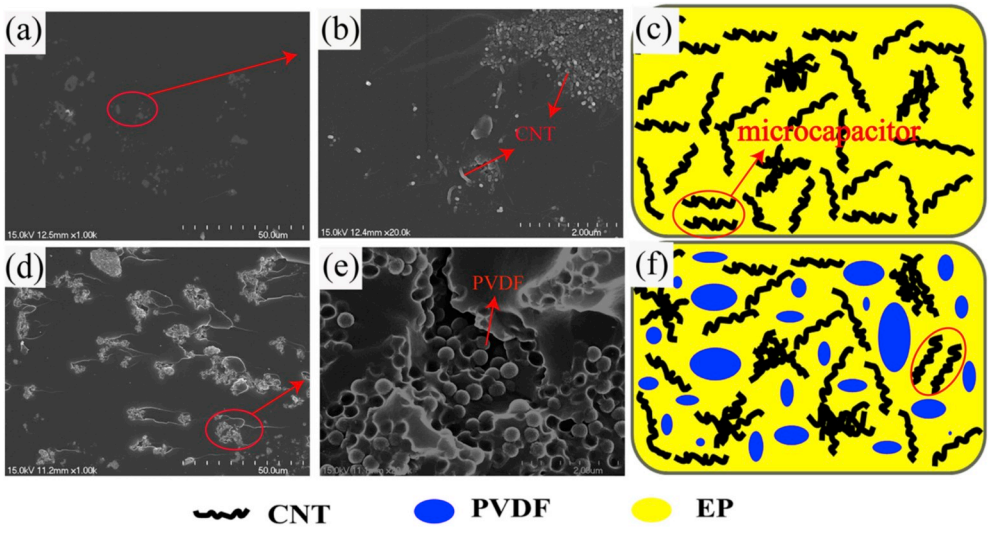

Fig. 3. SEM images of fracture surfaces of CNT/EP (a, b and c) and CNT/PVDF/EP (d, e and f) composites (f_{CNT} = 0.34 wt%).

3.3. Spatial distribution of MWCNTs in composites

Properties of composites are closely related to the dispersion of inorganic fillers [31]. SEM images of cross-sections of CNT/EP and CNT/PVDF/EP composites etched using 1, 4-dioxane are shown in Fig. 3. There are significant agglomerates of CNTs in CNT/EP composites (Fig. 3a, b and 3c). The same phenomenon is also found in CNT/PVDF/EP, moreover there are larger spherical agglomerates (Fig. 3d, e and 3f), which are proved to be PVDF powders using EDS data (Figure S1). However, no CNTs are found in PVDF phase of CNT/PVDF/EP. Several factors are responsible for above results. One is that PVDF and EP are incompatible; the second is that good solvent for PVDF is not used in the mixing process, and the third is that curing temperature is lower than melting point of PVDF. Therefore, PVDF always exists in powder form, and CNTs cannot enter the inside or the surface of PVDF, further demonstrating that there is no interaction between PVDF powders and CNTs when bad solvent is used.

fPCNT has so low density (30–34 mg/cm^3) that can be supported by a dandelion (Fig. 4a). After infiltrated with EP resin, fPCNT retains its 3D continuous network in fPCNT/EP composites (Fig. 4b and c). As electron-deficient PVDF is adsorbed on surfaces of electron-rich CNTs during the preparing process of fPCNT, so CNTs are uniformly distributed in PVDF phase in fPCNT/EP as shown in SEM images (Figure S2).

3.4. Conductivities and f_c values of composites

Fig. 5 shows frequency dependence of AC conductivity for different composites. The electrical conductivity increases as either frequency or CNT content (f) increases, however, specific f values for reaching the conductivity transition of three kinds of composites in low frequency region are different. Using the least square method to fit conductivities of composites at 100 Hz, f_c values of CNT/EP, CNT/PVDF/EP and fPCNT/EP composites were calculated to be 0.34, 0.38 and 0.25 wt%, respectively (Fig. 6). This difference in conductivity is related to the spatial distribution of conductors in composites. Compared with CNT/EP, CNTs and PVDF in CNT/PVDF/EP are dispersed in EP, so the existence of PVDF hinders the formation of conductive network. In fPCNT/EP composite, CNTs are dispersed in PVDF and form three-dimensional framework, these are good for forming conductive path at lower f.

3.5. Dielectric properties and mechanism of composites

Fig. 7 displays frequency dependence of Dk of different composites. As f increases, Dk of each kind of composites increases to the maximum Dk (ε_{max}) and then decreases, this is the typical phenomenon of conductor/polymer composites. With same f and PVDF loading, fPCNT/EP composite has higher Dk than CNT/PVDF/EP; moreover, the former gets higher ε_{max} at lower f than CNT/EP and CNT/PVDF/EP composites. When f is 0.25 wt%, the Dk of fPCNT/EP can also reach about 170. These data show that fPCNT/EP composite can achieve higher Dk at lower f. Since Dk of EP, PVDF/EP and fPVDF are all less than 5 (Fig S3), it can be concluded that the three-dimensional framework not only reduces f_c of composites, but also greatly increases Dk.

Dk of a conductor/polymer composite depends on microcapacitance and spatial polarization. For a composite based on CNTs and polymer, when electric field was applied on both sides of the composite, an adjacent pair of CNTs will form a microcapacitor, in which CNTs act as two electrodes and the polymer between CNTs acts as a medium [32]. As f increases, more capacitors tend to be formed in composite; while agglomerations of CNTs also increase, this is not beneficial to form microcapacitors. Fig. 8 show that fPCNT/EP has the largest capacitance among all composites with same f. This is because good solvent of PVDF was used to prepare fPCNT, so PVDF molecular chains can be adsorbed on surfaces of CNTs. This not only reduces the agglomeration of CNTs, but also increases the ability of forming more microcapacitors. In CNT/EP and CNT/PVDF/EP composites, CNTs have poor dispersion and do not interact with EP and PVDF.

It is worth noting that when three composites have same Dk, fPCNT/EP has smaller capacitance than CNT/EP and CNT/PVDF/EP, meaning that besides the enhancement of microcapacitance, interfacial polarization is another important factor for increasing Dk of fPCNT/EP.

For a composite based on CNTs and polymer, when an electric field is applied, positive charges will accumulate in the polymer near CNTs, while negative charges will accumulate on the surfaces of CNTs, this accumulation process of positive and negative charges will result in interface polarization [33]. Due to different spatial structures, three composites have different interface polarization. The strength of interfacial polarization depends on the difference in conductivity between two phases. Greater difference in conductivity brings stronger interfacial polarization effect [34]. CNT/EP has interfacial polarization at the interface between CNTs and EP, while interfacial polarization exists at interfaces of CNT-PVDF, CNT-EP and PVDF-EP in CNT/PVDF/EP. Since PVDF has larger Dk than EP, CNT-PVDF has weaker interfacial polarization than CNT-EP, so CNT/PVDF/EP has smaller overall interfacial polarization than CNT/EP with the same f. fPCNT/EP has not only interfacial polarization caused by the dispersion of CNTs in PVDF phase, but also interfacial polarization at the interface between fPCNT and EP, the latter does not exist in CNT/EP and CNT/PVDF/EP composites. In addition, compared with PVDF in CNT/PVDF/EP, PVDF in fPCNT/EP exhibits β phase, which has higher Dk [28], this is beneficial to improve the interface polarization between fPCNT and EP. Therefore, among all composites with the same f, fPCNT/EP has the largest capacitance and greatest interfacial polarization, leading to the largest Dk.

Fig. 9 displays the frequency dependence of dielectric loss of different composites. As f increases, the dielectric loss of three composites increases and jumps near f_c. For a conductor/polymer composite, its dielectric loss is generally composed of conduction loss (suitable for very low frequencies) and polarization loss of space charge [35]. When f approaches f_c, fPCNT/EP has much smaller dielectric loss than CNT/EP and CNT/PVDF/EP. At each f_c, the dielectric losses of CNT/EP, CNT/PVDF/EP and fPCNT/EP are 100, 75 and 0.5 (100 Hz), respectively. This is because CNTs mainly present as agglomerates in CNT/EP and CNT/PVDF/EP composites, causing very high polarization loss. In fPCNT/EP, although the conductive path is formed, PVDF is adsorbed on

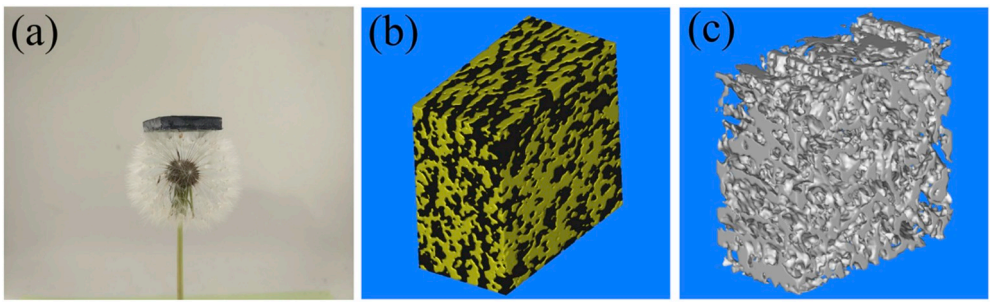

Fig. 4. Digital photos of fPCNT on a dandelion (a), 3D micro-CT images of fPCNT/EP composite (b) and 3D micro-CT images without EP resin (c).

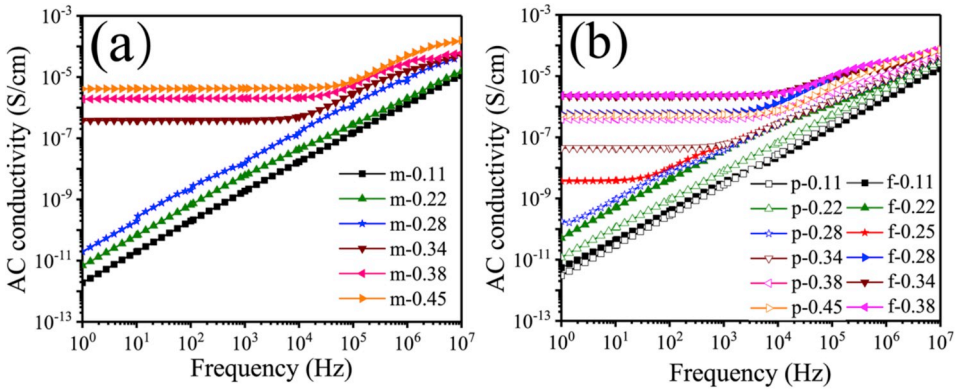

Fig. 5. Frequency dependence of AC conductivity for CNT/EP composite (a), CNT/PVDF/EP and fPCNT/EP (b) composites.

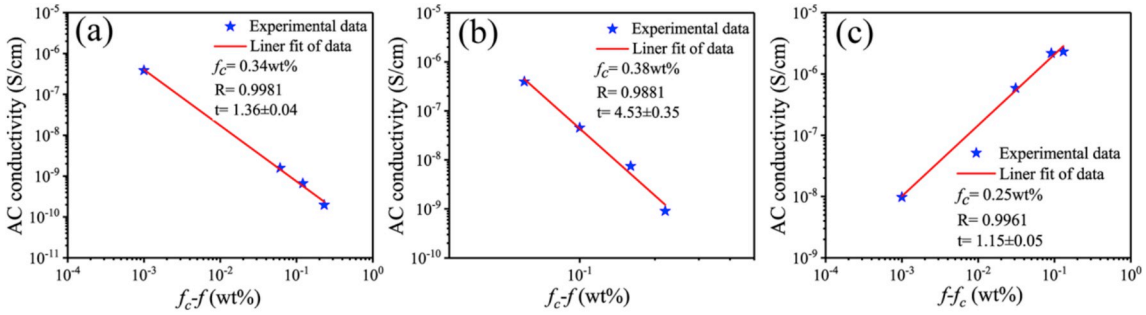

Fig. 6. Log−log plots of conductivity at 100 Hz VS ($f - f_c$) of CNT/EP (a), CNT/PVDF/EP (b) and fPCNT/EP (c) composites.

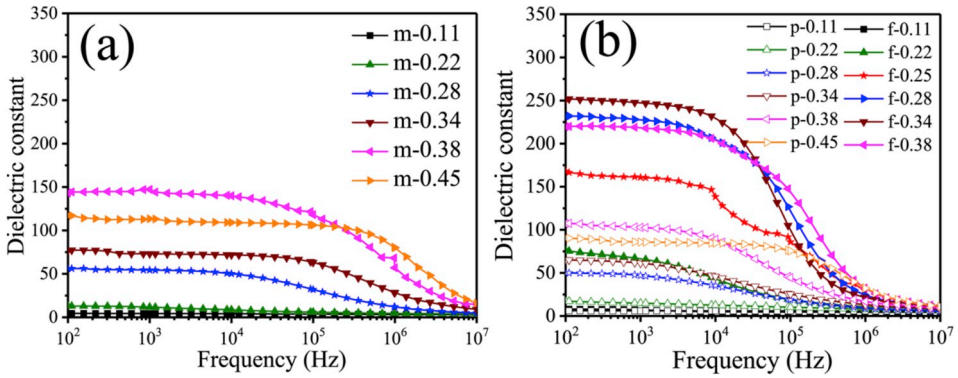

Fig. 7. Frequency dependence of dielectric constant for CNT/EP (a), CNT/PVDF/EP and fPCNT/EP (b) composites.

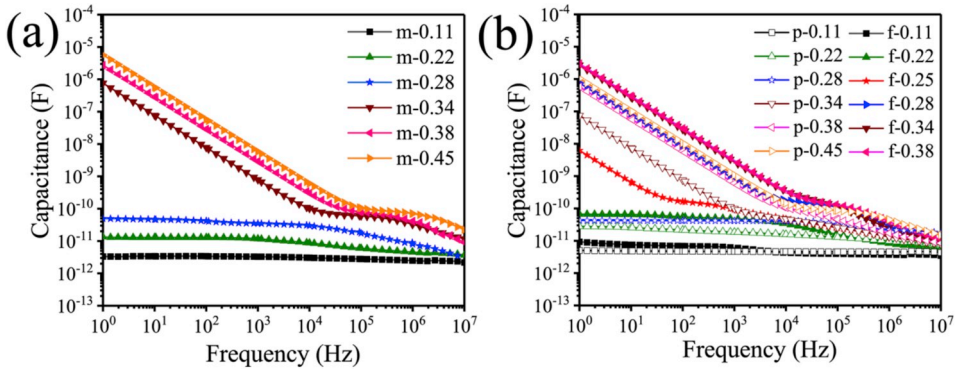

Fig. 8. Frequency dependence of capacitance for CNT/EP (a), CNT/PVDF/EP and fPCNT/EP (b) composites.

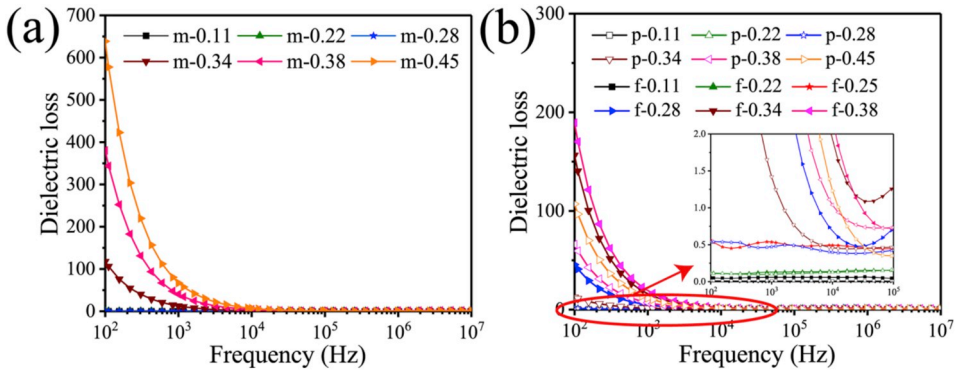

Fig. 9. Frequency dependence of dielectric loss for CNT/EP (a), CNT/PVDF/EP and fPCNT/EP (b) composites.

surfaces of CNTs, leading to lower dielectric loss.

Cellulose polymers are widely used in preparing 3D-framework [36]. To verify the superiority of PVDF as framework binder, four CNT frameworks were prepared using four celluloses as framework binder. Dielectric properties of epoxy composites based on different frameworks (*f* of each composite was controlled at 0.25 wt%) are shown in Fig. 10, M20-CNT/EP and M450-CNT/EP have *Dk* of about 5 at 100 Hz, because the frameworks from M20 and M450 are so unstable that collapse takes place during the process of pouring EP resin into framework, and thus these corresponding composites show insulator property. fPCNT/EP, CNa-CNT/EP and CC-CNT/EP composites have greater *Dk* than CNT/EP (0.28 wt%, 100 Hz), demonstrating that 3D-framework plays an important role in imparting higher *Dk*. In addition, among five composites, fPCNT/EP composite has the highest *Dk* with best frequency stability, demonstrating the superiority of PVDF as binder for building 3D-framework and achieving good dielectric properties of composites. On one hand, the β-phase PVDF has the highest *Dk* compared to other binders; on the other hand, the electron-deficiency endows PVDF with unique ability to form a donor-acceptor complex on surfaces of CNTs, so CNTs have good dispersion and thus forming more microcapacitors.

3.6. Equivalent circuits of composites

To reveal the mechanism behind different dielectric properties of different composites, impedance curves of these composites were simulated using ZsimpWin software. CNT/EP and CNT/PVDF/EP composites can be represented by same equivalent circuit (Fig. 11a), proving that their mechanism behind dielectric properties are similar, further indicating that PVDF powders act as one part of matrix. fPCNT/EP composites need to be simulated with different equivalent circuit (Fig. 11 b) from CNT/EP and CNT/PVDF/EP composites, indicating that fPCNT/EP has different nature for dielectric properties.

Compared to CNT/EP and CNT/PVDF/EP composites, fPCNT/EP has

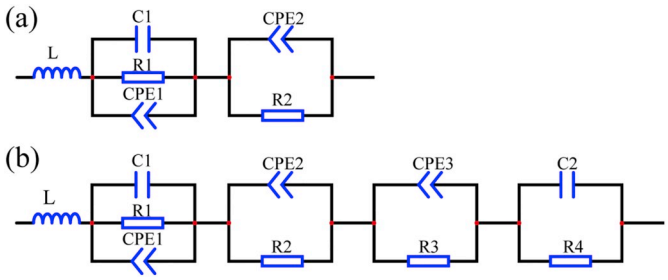

Fig. 11. Equivalent circuits of CNT/EP, CNT/PVDF/EP (a) and fPCNT/EP (b) composites.

additional two parallel circuits, suggesting that the composite contains two factors that affecting dielectric properties. On the one hand, the formation of the donor-acceptor complex increases the dispersion of CNTs, thereby forming more microcapacitors. On the other hand, in fPCNT/EP composite, besides the interfacial polarization between CNTs and PVDF, there is interfacial polarization between fPCNT and EP.

Fig. 12 gives Nyquist plots of different composites. When *f* increases and reaches f_c of each kind of composites, the shapes of Nyquist plots of all composites change from line to semicircular shape, indicating the formation of conductive path. The magnitude of the semicircle diameter reflects the resistivity of a composite, and the larger the diameter is, the larger the resistance is [37]. Note that the center position of each circle is not on Y axis over the entire frequency range, so constant phase angle element (*CPE*) is introduced to obtain better fitting result [2].

Parameters from simulating results for composites are shown in Table S3-S5. With increasing *f* in composite, the total resistance (R_t) of composites decreases gradually, while the total capacitance (C_t) initially increases and then decreases as *f* increases in all composites, following

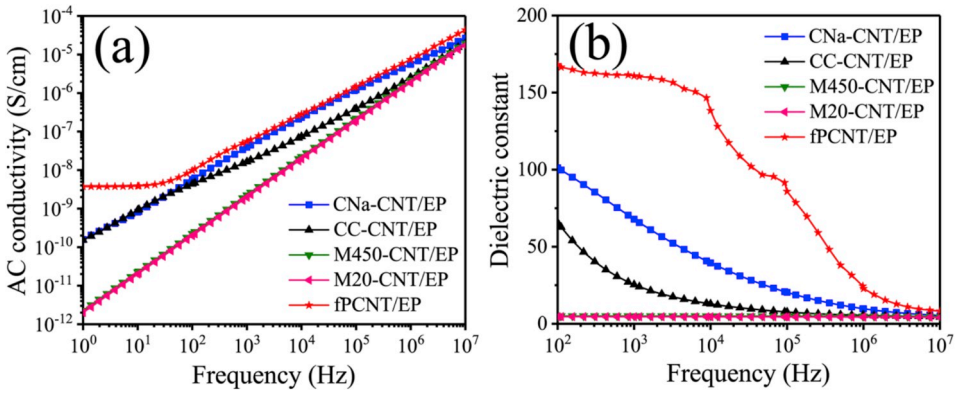

Fig. 10. AC conductivities (a) and dielectric constants (b) at different frequencies for composites with different framework binders.

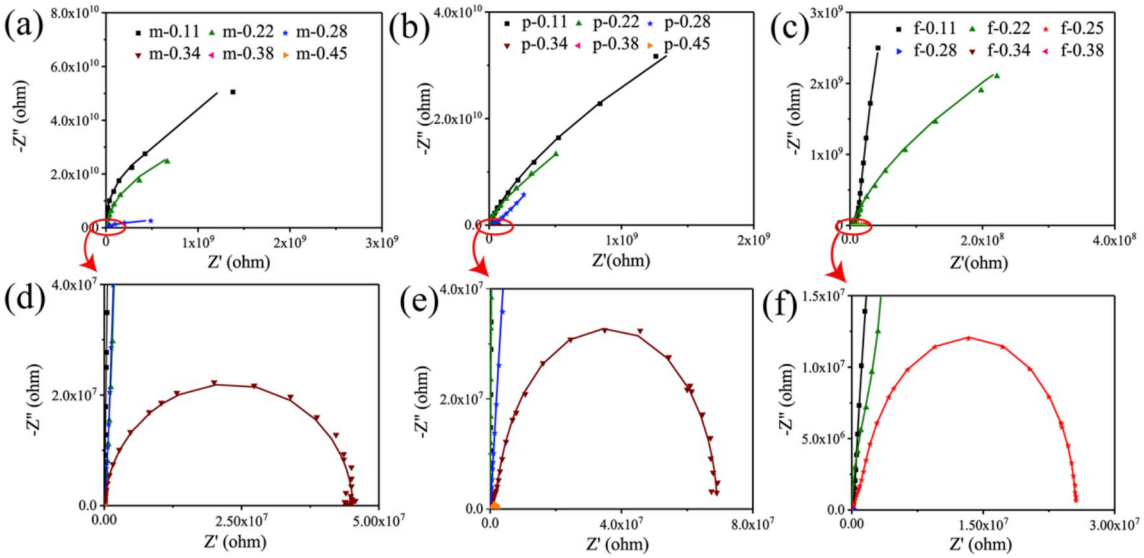

Fig. 12. Nyquist plots of CNT/EP (a, d), CNT/PVDF/EP (b, e) and fPCNT/EP (c, f) composites (solid symbols represent experimental data, solid lines are fitting results).

the general law of conductor/polymer composites [9]. Specifically, compared with CNT/EP and CNT/PVDF/EP, fPCNT/EP has larger C_t with same f. Better dispersion of CNTs brings the formation of the donor-acceptor complex and thus bigger chance of forming micro-capacitor. However, the theory of microcapacitance is not the sole reason for high Dk. As f increases, the interfacial polarization between fPCNT and EP is enhanced, and it becomes the main factor affecting dielectric properties of composites. Furthermore, fPCNT/EP has smaller R_t than CNT/EP and CNT/PVDF/EP because the three-dimensional framework of fPCNT is easy to constitute a conductive path in composites.

4. Conclusion

Starting from α-phase PVDF (binder) and CNTs (conductor), a novel three-dimensional framework (fPCNT) has been developed using ice template method, and PVDF in fPCNT contain both α and β phases. The f_c of fPCNT/EP composite is as low as 0.25 wt%, much lower than those of CNT/EP (0.34 wt%) and CNT/PVDF/EP (0.38 wt%). For fPCNT/EP composite with 0.25 wt% CNTs, its Dk reaches 170 (100 Hz), much higher than the values of CNT/EP and CNT/PVDF/EP even f of two controls is bigger (0.28 wt%). fPCNT simultaneously endows fPCNT/EP composites with higher capacitance and stronger spatial interface polarization, these two factors are responsible for outstanding dielectric properties of fPCNT/EP composites.

Acknowledgments

We thank National Natural Science Foundation of China (51873135), Key Major Program of Natural Science Fundamental Research Project of Jiangsu Colleges and Universities (18KJA430013) and Priority Academic Program Development of Jiangsu Higher Education Institution (PAPD) for supporting this project.

Appendix A. Supplementary data

Supplementary data to this article can be found online at https://doi.org/10.1016/j.compositesb.2019.04.042.

References

[1] Xu XL, Yang CJ, Yang JH, Wang Y. Excellent dielectric properties of poly (vinylidene fluoride) composites based on partially reduced graphene oxide. Compos B Eng 2017;109:91–100.
[2] Lu CQ, Yuan L, Guan QB, Liang GZ, Gu AJ. Optimizing ply pattern and composition of layered composites based on cyanate ester, carbon nanotube, and boron nitride: toward ultralow dielectric loss and high energy storage. J Phys Chem C 2018;122 (10):5238–47.
[3] Lu X, Zhang L, Tong Y, Cheng ZY. BST-P(VDF-CTFE) nanocomposite films with high dielectric constant, low dielectric loss, and high energy-storage density. Compos B Eng 2019;168:34–43.
[4] Hu JZ, Zhang L, Dang ZM, Wang DR. Improved dielectric properties of polypropylene-based nanocomposites via co-filling with zinc oxide and barium titanate. Compos Sci Technol 2017;148:20–6.
[5] Wang L, Piao X, Zou H, Wang Y, Li H. High dielectric, dynamic mechanical and thermal properties of polyimide composite film filled with carbon-coated silver nanowires. Appl Phys A 2014;118(1):243–8.
[6] Yaqoob U, Chung GS. Effect of surface treated MWCNTs and $BaTiO_3$ nanoparticles on the dielectric properties of a P(VDF-TrFE) matrix. J Alloy Comp 2017;695: 1231–6.
[7] Zhang L, Yuan S, Chen S, Wang D, Han B, Dang Z. Preparation and dielectric properties of core–shell structured Ag@polydopamine/poly(vinylidene fluoride) composites. Compos Sci Technol 2015;110:126–31.
[8] Wang Z, Cheng Y, Yang M, Huang J, Cao D, Chen S, Xie Q, Lou W, Wu H. Dielectric properties and thermal conductivity of epoxy composites using core/shell structured Si/SiO_2/polydopamine. Compos B Eng 2018;140:83–90.
[9] Liu C, Zheng LH, Yuan L, Guan QB, Liang GZ, Gu AJ. Origin of increasing dielectric constant at lower percolation threshold through controlling spatial distribution of carbon nanotubes in epoxy resin with microwave-assisted thermal curing technique. J Phys Chem C 2016;120(50):28875–85.
[10] Wang H, Zhang H, Zhao W, Zhang W, Chen G. Preparation of polymer/oriented graphite nanosheet composite by electric field-inducement. Compos Sci Technol 2008;68(1):238–43.
[11] Ding L, Liu L, Li P, Lv F, Tong W, Zhang Y. Dielectric properties of graphene-iron oxide/polyimide films with oriented graphene. J Appl Polym Sci 2016;133(12): 1–8.
[12] Chen GX, Li Y, Shimizu H. Ultrahigh-shear processing for the preparation of polymer/carbon nanotube composites. Carbon 2007;45(12):2334–40.
[13] Xu W, Ding Y, Jiang S, Zhu J, Ye W, Shen Y, Hou H. Mechanical flexible PI/MWCNTs nanocomposites with high dielectric permittivity by electrospinning. Eur Polym J 2014;59:129–35.
[14] Park C, Wilkinson J, Banda S, Ounaies Z, Wise KE, Sauti G, Lillehei PT, Harrison JS. Aligned single-wall carbon nanotube polymer composites using an electric field. J Polym Sci, Polym Phys Ed 2006;44(12):1751–62.
[15] Chang J, Liang GZ, Gu AJ, Cai S, Yuan L. The production of carbon nanotube/epoxy composites with a very high dielectric constant and low dielectric loss by microwave curing. Carbon 2012;50(2):689–98.
[16] P TA, SR J, S RRN. Comparative study of dielectric and mechanical properties of HDPE-MWCNT-SiO_2 nanocomposites. Mater Res Bull 2016;83:294–301.
[17] Zhang R, Han B, Fang D. New multifunctional porous Yb_2SiO_5 ceramics prepared by freeze casting. Ceram Int 2016;42(5):6046–53.

[18] Liu X, Rahaman MN, Fu Q. Bone regeneration in strong porous bioactive glass (13-93) scaffolds with an oriented microstructure implanted in rat calvarial defects. Acta Biomater 2013;9(1):4889–98.
[19] Wang Z, Shen X, Han N, Liu X, Wu Y, Ye W, Kim J. Ultralow electrical percolation in graphene aerogel/epoxy composites. Chem Mater 2016;28(18):6731–41.
[20] He F, Sui C, He X, Li M. Facile synthesis of strong alumina–cellulose aerogels by a freeze-drying method. Mater Lett 2015;152:9–12.
[21] Park OK, Lee JH. Carbon nanotube-poly(vinyl alcohol) hybrid aerogels: improvements in the surface area and structural stability by internal morphology control. Compos B Eng 2018;144:229–36.
[22] Guan F, Pan J, Wang J, Wang Q, Zhu L. Crystal orientation effect on electric energy storage in poly(vinylidene fluoride-co-hexafluoropropylene) copolymers. Macromolecules 2010;43(1):384–92.
[23] Von Seggern H, Fedosov SN. Conductivity-induced polarization buildup in poly (vinylidene fluoride). Appl Phys Lett 2002;81(15):2830–2.
[24] Tiwari V, Srivastava G. Structural, dielectric and piezoelectric properties of 0–3 PZT/PVDF composites. Ceram Int 2015;41(6):8008–13.
[25] Sarkar S, Garain S, Mandal D, Chattopadhyay KK. Electro-active phase formation in PVDF–$BiVO_4$ flexible nanocomposite films for high energy density storage application. RSC Adv 2014;4(89):48220–7.
[26] Singh P, Borkar H, Singh BP, Singh VN, Kumar A. Ferroelectric polymer-ceramic composite thick films for energy storage applications. AIP Adv 2014;4(8), 087117.
[27] Deville S, Saiz E, Nalla RK, Tomsia AP. Freezing as a path to build complex composites. Science 2006;311(5760):515–8.
[28] Dhand V, Hong SK, Lee HW. Fabrication of robust, ultrathin and light weight, hydrophilic, PVDF-CNT membrane composite for salt rejection. Compos B Eng 2019;160:632–43.
[29] Wise KE, Park C, Siochi EJ, Harrison JS. Stable dispersion of single wall carbon nanotubes in polyimide: the role of noncovalent interactions. Chem Phys Lett 2004; 391(4–6):207–11.
[30] Yang C, Lin Y, Nan C. Modified carbon nanotube composites with high dielectric constant, low dielectric loss and large energy density. Carbon 2009;47(4): 1096–101.
[31] Lee SH, Kontopoulou M, Park CB. Effect of nanosilica on the co-continuous morphology of polypropylene/polyolefin elastomer blends. Polymer 2010;51(5): 1147–55.
[32] Fan PF, Wang L, Yang JT, Chen F, Zhong M. Graphene/poly(vinylidene fluoride) composites with high dielectric constant and low percolation threshold. Nanotechnology 2012;23(36):365702.
[33] Sillars RW. The properties of a dielectric containing semiconducting particles of various shapes. Institution of Electrical Engineers-Proceedings of the Wireless Section of the Institution 1937;12(35):139–55.
[34] Zhou WY, Chen QG, Sui XZ, Dong LN, Wang ZJ. Enhanced thermal conductivity and dielectric properties of Al/β-SiCw/PVDF composites. Compos Part A-Appl S 2015;71:184–91.
[35] Vo LT, Anastasiadis SH, Giannelis EP. Dielectric study of poly(styrene-co-butadiene) composites with carbon black, silica, and nanoclay. Macromolecules 2011;44(15):6162–71.
[36] Zheng TT, Li A, Li ZY, Hu WB, Shao L, Lu LB, Cao Y, Chen YJ. Mechanical reinforcement of a cellulose aerogel with nanocrystalline cellulose as reinforcer. RSC Adv 2017;7(55):34461–5.
[37] Dang ZM, Yao SH, Yuan JK, Bai JB. Tailored dielectric properties based on microstructure change in $BaTiO_3$-carbon nanotube/polyvinylidene fluoride three-phase nanocomposites. J Phys Chem C 2010;114(31):13204–9.